Thrust Measurement for Large-scale Helicon Plasma Thruster Using Multiple Antennas

IEPC-2015-413／ISTS-2015-b-413

Presented at Joint Conference of 30th International Symposium on Space Technology and Science 34th International Electric Propulsion Conference and 6th Nano-satellite Symposium, Hyogo-Kobe, Japan July 4 – 10, 2015

S. Tonooka[1]
The Graduate University for Advanced Studies, Sagamihara, Kanagawa, 252-5210, Japan

I. Funaki[2], T. Matsuoka[3]
Japan Aerospace Exploration Agency, Sagamihara, Kanagawa, 252-5210, Japan

S. Iwabuchi[4], T. Nakamura[5], S. Shinohara[6], H. Nishida[7]
Tokyo University of Agriculture and Technology, Koganei, Tokyo, 184-8588, Japan

Operation of present electric propulsion such as ion thrusters has lifetime limitation due to electrode erosion. Future missions such as interplanetary flight and manned flight to the mars require high power and high thrust. These requirements make the lifetime issue severe. In order to solve the problem, we have been studied advance electric propulsion system by use of helicon plasma sources with Lissajous acceleration. In our previous work, experiments of plume investigation and thrust measurements were carried out. In this study, thrust measurement with Lissajous acceleration for large-scale 100 mm diameter thruster was conducted. When powering the Lissajous acceleration stage, a slight increase in thrust is observed at high power region. The variation in thrust is observed when the phase between RF pulses in acceleration stage is changed. Thrust, specific impulse, thrust efficiency (thrust power/input power) are ? mN, ? s, and ?%, at a total input power of ? kW (? kW for plasma generation and ? kW for acceleration), respectively.

Nomenclature

B_z	=	Axial magnetic field
c_s	=	Ion sound velocity
HDLT	=	Helicon Double Layer Thruster
PM-HDLT	=	Permanent Magnet HDLT
HEAT	=	Helicon Electrodeless Advanced Thrusters
I	=	r.m.s. RF current
I.D.	=	Inner Diameter
Fy	=	Y component of the resultant pressure force acting on the vehicle
LHPD	=	Large Helicon Plasma Device

[1] Graduate Student, Department of Space and Astronautical Science, tonooka@ac.jaxa.jp.
[2] Associate Professor, Institute of Space and Astronautical Science, funaki@isas.jaxa.jp.
[3] Researcher Fellow, Institute of Space and Astronautical Science, takeshi.matsuoka1@ppc.osaka-u.ac.jp
[4] Graduate Student, Department of Mechanical System Engineering, iwabuchi.s.ab@m.titech.ac.jp.
[5] Graduate Student, Department of Mechanical System Engineering, 50012833007@st.tuat.ac.jp.
[6] Professor, Tokyo University of Agriculture and Technology, sshinoha@cc.tuat.ac.jp.
[7] Associate Professor, Tokyo University of Agriculture and Technology, hnishida@cc.tuat.ac.jp.

M	=	Ion mass
P_{in}	=	RF input power
P_{abs}	=	Absorbed RF power by plasma
RF	=	Radio frequency
T_e	=	Electron temperature
VASIMR	=	Variable Specific Impulse Magnetoplasma Rocket
Z	=	Impedance
κ	=	Boltzmann constant

I. Introduction

For deep space missions, high specific impulse and a long lifetime are required. Electric propulsion [1] can meet those requirements. Combination of a helicon plasma production and electro-magnetic plasma acceleration which is powered by radio frequency waves could be a solution because the entire process is achieved with no physical contact between the plasma and electrodes. Various schemes have been developed to realize electrodeless electric propulsion: VASIMR [2], HDLT [3], and others [4].

We have been studying Lissajous acceleration method [5][6], one of the electrodeless thrusters, whose concept is shown in Fig.1. This study becomes a part of the HEAT (Helicon Electrodeless Advanced Thrusters) project [7]. The thruster consists of two sections, a plasma generation section by helicon plasma discharge and a plasma acceleration section by the Lissajous method. In the acceleration section, rotating electric fields are applied to the plasma in order to excite electron azimuthal currents. The Lorentz force, which is the product of the currents and the static magnetic field, accelerates plasma and produces thrust.

In our previous work, experiments of plume investigation were carried out and preliminary thrust measurement was conducted [8][9]. Thrust by this Lissajous method is not measured directly, and therefore the thruster performance is unknown. In this paper, we report thrust measurement experiments for helicon plasma thruster with Lissajous acceleration.

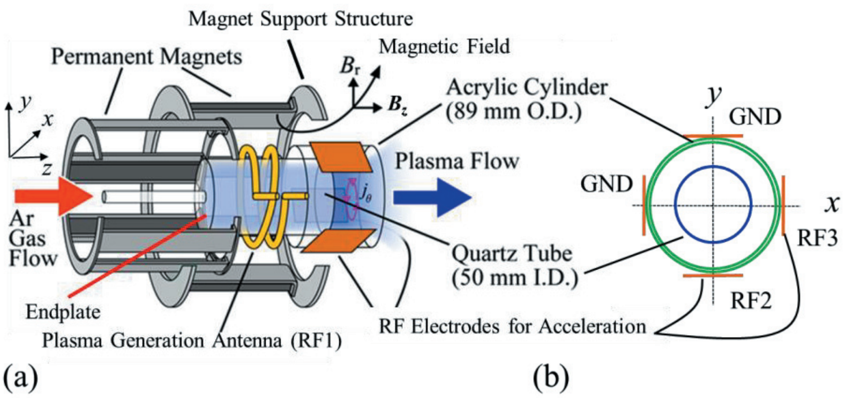

Figure 1. Laboratory model of Helicon thruster with Lissajous accelerator.
(a) side voew and (b)front view of thruster.

II. Experimental Setup and Method

The styles and formats for the 34th IEPC Template have been incorporated into the structure of this document. If you are using Microsoft Word 6.0 or later, please use this template to prepare your manuscript. A template for LaTEx is available separately. Please upload a PDF version of the final typeset manuscript.

A. Experimental Setup

Experiments are conducted by the use of the "Large Helicon Plasma Device" (LHPD) [10] in the Institute of Space and Astronautical Science (ISAS). Experimental set up is shown in Fig.2. As shown in Fig.2, a quartz tube was placed inside the LHPD. Thrust is measured by a pendulum type thrust stand which is mentioned in section B below. Other experimental parameters are shown in Table I and configuration for power supply is shown in Fig.3. Pulse high frequency (9.5 MHz) discharge (200 ms) was input to double loops generating antenna (RF1) in all conditions. Dimensions of comportments for thrusters and the positions are shown in Fig.4. Gas mass flow is controlled by mass flow controller (HORIBA STEC, SEC-E440J) and monitored by mass flow controller monitor unit (KOEFLOC 3660). Input power is measured at monitor port of matching box (THAMWAY, T161-6013H-TN) by oscilloscope (Tektronix, TDS2014)

Table 1. Experimental Parameters.

Quartz Tube Dimensions	Helicon plasma source w/o Lissajous acceleration	Helicon plasma source w/ Lissajous acceleration
RF Frequency	9.5 MHz	9.5 MHz
Input Power for generating antenna	1.3- 1.9 kW	1.0 kW
Input Power for acceleration antenna	-	0.5- 1.5 kW
Duration of RF Pulse	~200 ms	~200 ms
Phase between RF2 and RF3	-	0°, 90°
Chamber Pressure Before Discharge at Ar Flow of 0.89 mg/s	$< 2\times10^{-2}$ Pa	$< 2\times10^{-2}$ Pa
Gas mass flow	20, 30, 50, 70 sccm	20, 30, 50, 70 sccm

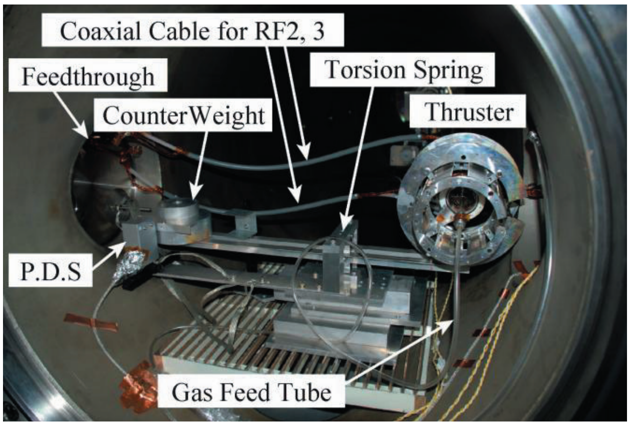

Figure 2. Configuration of thrust measurement.
(In case of thruster size 50 mm I.D.)

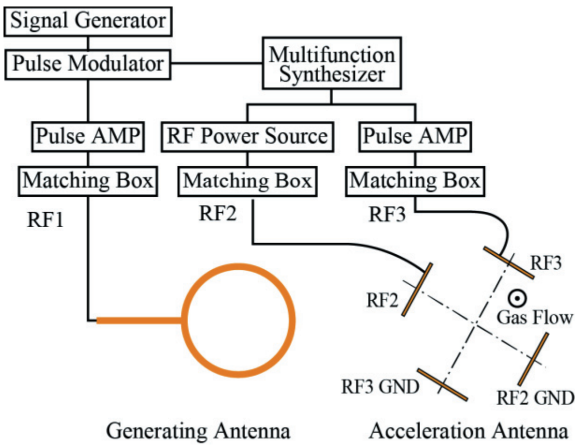

Figure 3. Configuration of power supply

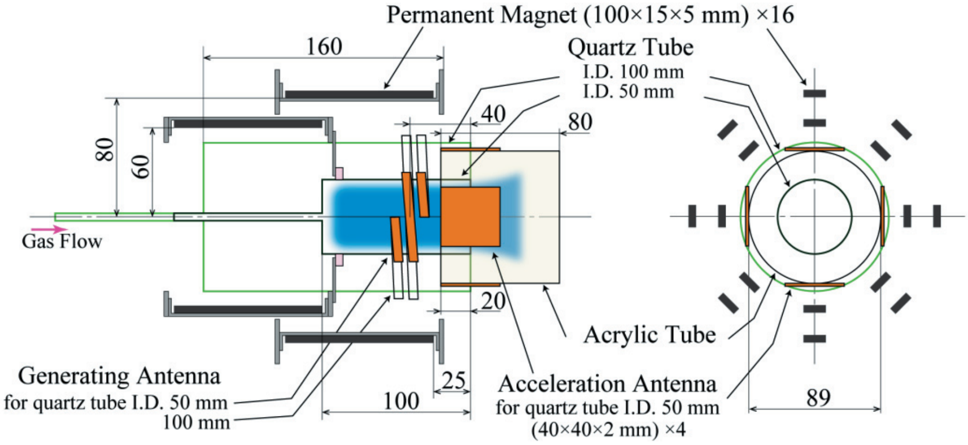

Figure 4. Dimensions for helicon thruster

(a) side view and (b)front view of thruster.

B. Antennas and RF setup

An double loops antenna (RF1) is placed around the quartz tube in generating stage and pulse high frequency (9.5 MHz) discharge (200 ms) was input in all conditions. The diameter of an double loop antenna is 110mm and has no contact with the thruster.

An accelerating stage is added in order to excite rotating electric fields based on the Lissajous Acceleration Method (Section 1). Four flat copper antennas are placed on acrylic tube as surrounding a thruster (Figs. 11(a) and 11(b)). The shape of the acceleration antennas is a 40 mm square with 2 mm thick. Four acceleration antennas are placed evenly on an 89 mm circle as shown in Fig. 11(b). Two of the antennas are powered by 13.56 MHz RF pulses. Relative phase of the two 13.56 MHz pulses can be changed by multifunction synthesizer in order to generate rotating electric fields.

All RF antennas are separated from the thruster structure. We confirmed that no impulse above noise level is observed without propellant gas flow. Therefore, force between RF antennas and the thruster structure can be neglected. The experimental parameters are shown in Table II.

C. Thrust stand

Thrust stand is a micro thrust measurement system based on the pendulum method as shown in Fig.5. Two FLEXI-HINGEs (SDP/SI, S99FXS-031220) are used as a pivot of the pendulum. When the thruster produces the thrust, an impulse is imparted to the pendulum. This impulse drives damped oscillations of the pendulum as shown in Fig.0. The oscillation is detected by a photo displacement sensor (Omron, Z4D-F04A). An electromagnetic damper by the use of permanent magnets is placed to adjust the damping rate of the oscillation amplitude. In order to keep the balance of the thrust stand and increase the sensitivity of the thrust stand, counter weights are placed to cancel the gravitational force which acts on the thruster. Acceleration antennas (Fig.1) are suspended as surrounding the quartz tube contactlesslly and both the tube and circuit are mounted on the stand. Due to the fact that electromagnetic thrust and thermal thrust is given to the circuit and the tube, the sum of the electromagnetic thrust and thermal thrust is measured by the thrust stand.

The response of the thrust stand to applied impulses is calibrated by striking a steel ball. The peak amplitude of the oscillation is proportional to the applied impulse ($I_{bit}= Cd_a$) with a fitting coefficient of C. the thrust is estimated by $F = I_{bit}/\tau$, assuming a constant thrust during thruster operation duration (τ=200ms).

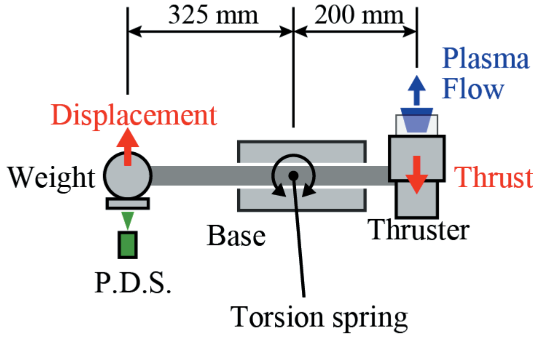

Figure 5. Experimental setup of thrust stand for thrust measurement.

III. Experimental Results and Discussion

The thrust, specific impulse for the 100 mm I.D. tube is shown in Fig.6 as a function of the mass flow rate for each input power. The maximum thrust (11 $\pm$0.66 mN) was measured at a parameter set: the mass flow rate of 70 sccm and input power of 1.3~1.5 kW. The maximum specific impulse (8.4×10^2 $\pm$33 s) was measured at a parameter set: the mass flow rate of 10 sccm and input power of 1.3~1.5 kW. The plasma ignition was not stable for the experimental parameters set of high gas mass flow and low input power. To elucidate the dependence of thrust characteristics for mass flow rate and input power, Fig.7 and Fig.8 are prepared. Fig.7 is the thrust and specific impulse for various gas flow rate (input power 1.3~1.9 kW). The thrust is proportional to the mass flow rate at a given input power. In addition, with the gas mass flow rate increase the brighter emission is observed. This suggests that the increase of the thrust could be caused by increase of the plasma density in the quartz tube. However, specific impulse decreases with increasing of gas mass flow. This indicates the rate of the thrust increase to gas mass flow increase is not enough to improve the specific impulse. Fig.8 shows the thrust and the specific impulse for the various input power (gas mass flow 30 sccm). Both the thrust and specific impulse are proportional to the input power. However, a rate of the thrust increase gradually decreases with increasing input power. Since the input power was measured at the output of a matching box, power loss through the coaxial cable from the matching box to the generating antenna (Fig.3) can be considered. The best performance is summarized in Table II in conclusion section.

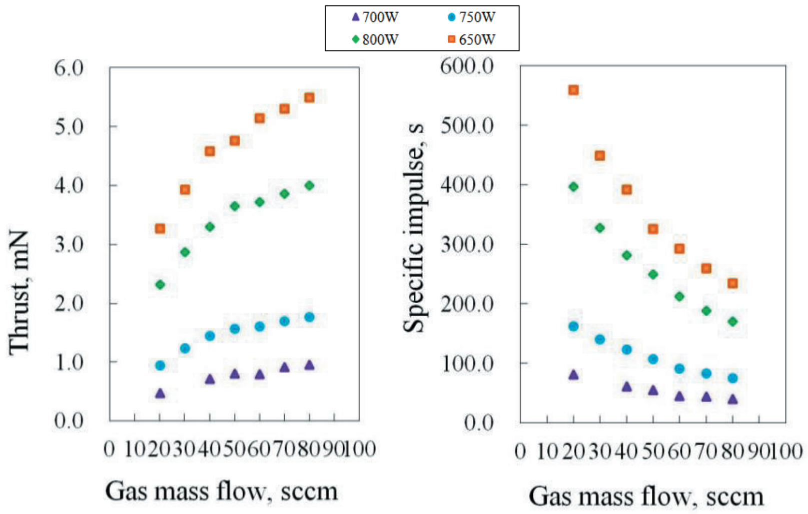

Figure 6. Thrust characteristics for 100 mm I.D. w/o Lissajous

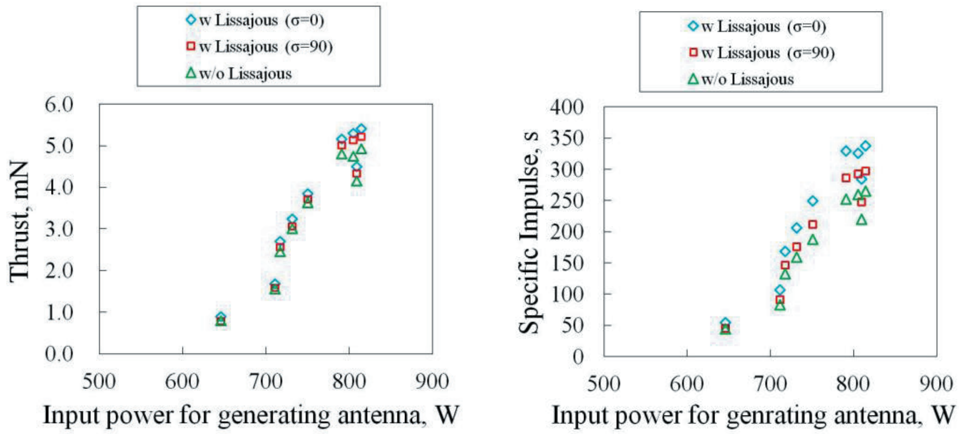

Figure 9. Thrust Performance as function of relative phase between RF2 and RF3.
(*input power to the accelerating antenna 1.5 kW , gas mass flow 50 sccm)*

As shown in Fig.?, When powering the Lissajous acceleration antenna, a slight increase in thrust is observed in every experimental condition. The thrust increase is clear at high power region and 11% increase at 800 W for acceleration antenna. Specific impulse is also improved by input acceleration antenna. The maximum thrust is 5.4 mN and maximum specific impulse is 340 s. The variation in thrust is observed when the phase between RF pulses in acceleration stage is changed. As shown in Fig.?, maximum thrust is observed in σ=0. The relative phase between RF2 and RF3 is fixed at the multifunction synthesizer.

Thrust, specific impulse, thrust efficiency (thrust power/input power) are ? mN, ? s, and ?%, at a total input power of ? kW (? kW for plasma generation and ? kW for acceleration), respectively.

Relative phase between RF2 and RF3 is fixed at the multifunction analyzer.
This implies that the thermal thrust dominates thrust over the Lissajous acceleration.

IV. Conclusion

Thrust measurement for helicon plasma thruster with multiple antennas was conducted in large scale thruster size (I.D. 100 mm) and thrust characteristics were evaluated. Improvements in thrust performance were observed by powering acceleration antenna. Compared to w/o Lissajous, maximum thrust (11 ± 0.66 mN) was 11% increase and maximum specific impulse ($8.4 \times 10^2 \pm 33$ s) was 30% increase each. The best performance is summarized in Table II. Both the thrust and specific impulse increased by powering acceleration antenna. However, with increasing the gas flow rate, the thrust increased and specific impulse decreased. Same trend was observed for two different thruster sizes.

Thrust increasing was observed in high power region.

Extra power for accelerating antenna is

The incease of thrust is smaller than theoretical thrust.

Acknowledgments

This work was supported by the Grants-in-Aid for Scientific Research under Contract No. (S) 21226019 from the JSPS.

References

[1]Vatistas, G. H., Lin, S., and Kwok, C. K., "Reverse Flow Radius in Vortex Chambers," *AIAA Journal*, Vol. 24, No. 11, 1986, pp. 1872, 1873.

[2]Dornheim, M. A., "Planetary Flight Surge Faces Budget Realities," *Aviation Week and Space Technology*, Vol. 145, No. 24, 9 Dec. 1996, pp. 44-46.

[1]Robert G., JAHN: Physics of Electric Propulsion, (MacGraw-Hill, Inc., New York, 1968).

[2]Chang Diaz, F. R., "The VASIMR Rocket," Scientific American, November 2000, Vol. 283, No. 5, 2000, pp., 90, 97.

[3]Williams, L. T., Walker, M. L. R., "Thrust Measurements of a Helicon Plasma Source," *47th AIAA/ASME/SAE/ASEE Joint Propulsion Conference & Exhibit,* AIAA2011-5893, Jul. 31-Aug. 3, San Diego, 2011.

[4]Yasaka, Y., Nishino, S., Yamamoto, M., Nakamoto, S., Takeno, H., Yonemori, H., "Novel Control of Magnetoplasma Thruster by Using a Rotating RF System," *49th AIAA Aerospace Sciences Meeting including New Horizons Forum and Aerospace Exposition*, AIAA2011-1072, Jan. 4-7, Orland, 2011.

[5]Toki, K., Shinohara, S., Tanikawa, T., Shamrai, K. P., and Funaki, I., "Preliminary Investigation of Helicon Plasma Source for Electric Propulsion Applications," 28th International Conference on Electric Propulsion, IEPC-2003-0168, Toulouse, 2003.

[6]Nishida, H., Shinohara, S., Tanikawa, T., Hada T., Funaki I., Matsuoka T., Shamrai, K. P., and Motomura, T., "Preliminary Study on Electrodeless Magneto-Plasma-Dynamic Thruster Using a Helicon Plasma Source," *46th AIAA/ASME/SAE/ASEE Joint Propulsion Conference & Exhibit*, AIAA-2010-7013, Nashiville, 2010.

[7]Shinohara, S., Nishida, H., Yokoi, K., Nakamura, T., Tanikawa, T., Hada, T., Otsuka, F., Motomura, T., Ohno, E., Funaki, I., Matsuoka, T., Shamrai, K. P., and Rudenko, T. S., "Research and Development of Electrodeless Plasma Thrusters Using High-Density Helicon Sources: The Heat Project," *32nd International Electric Propulsion Conference*, IEPC-2011-056, Sept.11-15, Wiesbaden, Germany, Sept. 2011.

[8]T. Matsuoka, I. Funaki, K.P. Shamurai, S. Satoh, T. Fujino, S. Iwabuchi, T. Nakamura, H. Nishida, S. Shinohara, T. Hada, and T. Tanikawa, Laboratory Model Development of Electrodeless Helicon Plasma Thruster Using Permanent Magnet, IEEE Transaction on Plasma Science, submitted.

[9]T. Nakamura, H. Nishida, S. Shinohara, I. Funaki, T. Tanikawa, S. Iwabuchi, T. Hada, Experimental Investigation of Thrust Characteristics in Lissajous Acceleration Type Electrodeless Helicon Plasma Thruster, 29th ISTS, 2013-o-1-08, Nagoya,June 2-9, 2013.

[10]Tanikawa, T., and Shinohara, S., "Plasma performance in very large helicon device," *Thin Solid Films*, Vol. 506-507, 2006, pp., 559, 563.

[11]T. Matsuoka, I. Funaki, K. P. Shamrai, S. Satoh, T. Hujino, S. Iwabuchi, T. Nakamura, H. Nishida, S. Shinohara, T. Hada, T. Tanikawa, "Comparison of Simulated Plasma Flow Field in a Two-Dimensional Magnetoplasmadynamic Thruster With Experimental Data." *IEEE*, (2013).